AMERICAN SOCIETY FOR MICROBIOLOGY | Journal of Virology®

Murine Olfactory Bulb Interneurons Survive Infection with a Neurotropic Coronavirus

D. Lori Wheeler,[a] Jeremiah Athmer,[b] David K. Meyerholz,[c] Stanley Perlman[a,b]

Interdisciplinary Graduate Program in Immunology,[a] Department of Microbiology and Immunology,[b] and Department of Pathology,[c] University of Iowa, Iowa City, Iowa, USA

ABSTRACT Viral infection of the central nervous system (CNS) is complicated by the mostly irreplaceable nature of neurons, as the loss of neurons has the potential to result in permanent damage to brain function. However, whether neurons or other cells in the CNS sometimes survive infection and the effects of infection on neuronal function is largely unknown. To address this question, we used the rJHM strain (rJ) of mouse hepatitis virus (MHV), a neurotropic coronavirus that causes acute encephalitis in susceptible strains of mice. To determine whether neurons or other CNS cells survive acute infection with this virulent virus, we developed a recombinant JHMV that expresses Cre recombinase (rJ-Cre) and infected mice that universally expressed a silent (floxed) version of tdTomato. Infection of these mice with rJ-Cre resulted in expression of tdTomato in host cells. The results showed that some cells were able to survive the infection, as demonstrated by continued tdTomato expression after virus antigen could no longer be detected. Most notably, interneurons in the olfactory bulb, which are known to be inhibitory, represented a large fraction of the surviving cells. In conclusion, our results indicated that some neurons are resistant to virus-mediated cell death and provide a framework for studying the effects of prior coronavirus infection on neuron function.

IMPORTANCE We developed a novel recombinant virus that allows the study of cells that survive an infection by a central nervous system-specific strain of murine coronavirus. Using this virus, we identified neurons and, to a lesser extent, nonneuronal cells in the brain that were infected during the acute phase of the infection and survived for approximately 2 weeks until the mice succumbed to the infection. We focused on neurons and glial cells within the olfactory bulb because the virus enters the brain at this site. Our results show that interneurons of the olfactory bulb were the primary cell type able to survive infection. Further, these results indicate that this system will be useful for functional and gene expression studies of cells in the brain that survive acute infection.

KEYWORDS coronavirus, olfactory bulb, encephalitis, interneurons

Received 30 June 2017 **Accepted** 18 August 2017

Accepted manuscript posted online 23 August 2017

Citation Wheeler DL, Athmer J, Meyerholz DK, Perlman S. 2017. Murine olfactory bulb interneurons survive infection with a neurotropic coronavirus. J Virol 91:e01099-17. https://doi.org/10.1128/JVI.01099-17.

Editor Rozanne M. Sandri-Goldin, University of California, Irvine

Address correspondence to Stanley Perlman, stanley-perlman@uiowa.edu.

Viral upper respiratory tract infection is a common cause of olfactory dysfunction, in part because the olfactory epithelium is located adjacent to the respiratory epithelium, the site of replication of multiple viruses that cause upper respiratory tract infection, and because olfactory neurons directly access the environment. Viruses take advantage of this direct connection with the olfactory bulb (OB) to enter the central nervous system (CNS) (1–6). In the process of gaining access to the CNS, these viruses damage the olfactory epithelium and the olfactory bulb, leading to altered olfaction (7–11).

The process of scent discrimination begins within the olfactory epithelium when odorants bind odorant receptors on olfactory sensory neurons (OSNs) (12, 13). OSNs

project their axons onto the dendrites of projection neurons (tufted cells and mitral cells) within the olfactory glomeruli of the OB. These tufted and mitral cells then send axons deeper into the brain, largely to the primary olfactory cortex, but also to secondary and tertiary connections of the OB. Interneurons within all the layers of the olfactory bulb modulate the signal sent by these projection neurons. While all olfactory bulb interneurons use gamma-aminobutyric acid as a neurotransmitter, some also express dopamine. These interneurons, which include granule cells and periglomerular cells, are characterized by soma size, soma location, dendrite extension, and expression of calcium-binding proteins (14–17). For example, periglomerular cells have a small soma; are located in the glomerular layer of the olfactory bulb; and express tyrosine hydroxylase, calbindin, or calretinin. In contrast, granule cells express calretinin but not calbindin or tyrosine hydroxylase (14, 18, 19). While these interneurons are inhibitory by nature, and anatomical studies have shown that each subtype extends dendrites, little is known about the functions of these cells or how they are molecularly distinct from each other.

Coronaviruses (CoV) are positive-stranded RNA viruses capable of causing disease in a variety of animals. These diseases range from respiratory, systemic, neurological, and gastrointestinal diseases in domestic, companion, and experimental animals to mild and severe respiratory disease in humans (20, 21). Neurotropic strains of the murine CoV, mouse hepatitis virus (MHV), cause acute encephalitis and acute and chronic demyelinating diseases of the central nervous system (22). Specifically, the nonrecombinant and recombinant (rJ) versions of neurotropic JHMV cause lethal encephalitis. When this virus is intranasally instilled, virus enters the CNS through the OB by direct infection of OSNs and anterograde transport via the olfactory nerve. Once in the OB, JHMV spreads *trans*-neuronally to connections of the main OB (23, 24). Unlike other neurotropic strains of MHV, JHMV primarily infects neurons (25–28). However, little is known about the ratio of neuronal to glial infection or about the subtypes of neurons infected by JHMV, although infection of tyrosine hydroxylase-expressing neurons may be limited to certain regions of the brain (24).

The irreplaceable nature of most neurons is a major factor in the long-term morbidity observed after viral infections of the central nervous system. Loss of individual neurons and the associated disruption of interconnected neural networks results in permanent damage to the brain. Though not extensively validated, it would be advantageous for neurons to survive after viral infection. In support of this, neurons have been shown to survive an attenuated rabies virus infection (29), but whether this phenomenon occurs with viruses other than attenuated rabies virus is not known.

Here, to study brain cells that survive infection after neurotropic CoV infection, we developed a recombinant JHM virus that expressed Cre recombinase (Cre). tdTomato mice contain a transgenic tdTomato cassette in a locus that is universally expressed (the *Rosa26* locus), thus allowing expression of the fluorescent protein tdTomato after Cre-LoxP-mediated excision of a stop cassette (30). Viral Cre expression within the infected host cell results in excision of a stop cassette, leading to expression of the red fluorescent protein tdTomato only in infected cells. Because the host cell contains the tdTomato cassette, cells surviving the infection permanently express tdTomato even after virus is eliminated. Using this model to assess survival of neurons after virus clearance, we identified a population of OB interneurons that survive the infection.

RESULTS

Construction of a Cre-expressing recombinant JHMV (rJ-Cre). Although it is established that rJ infects neurons, including mitral cells (25, 26), it is not known whether any neurons in general survive this infection or whether certain neuronal cell types preferentially survive. To engineer a Cre-expressing rJ virus, we used a previously described system of reverse genetics utilizing a bacterial artificial chromosome (BAC) cDNA clone (pBAC-JHMV^{IA}) (31). Cre was inserted into pBAC-JHMV^{IA} in place of open reading frame 4 (ORF4), a gene that is dispensable for viral replication in tissue culture or in mice (32, 33), using Red recombination with an arabinose-inducible Flp recom-

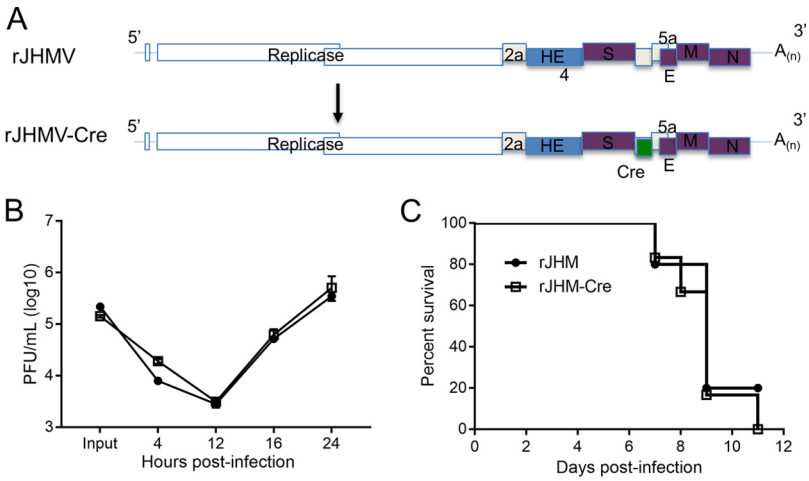

FIG 1 Characterization of Cre-expressing rJ. (A) Genomes of rJ and recombinant rJ expressing Cre recombinase. (B) Replication kinetics of rJ-Cre and rJ. 17Cl-1 cells were infected at an MOI of 0.1 PFU/cell. Virus titers were determined as described in Materials and Methods. (C) Mice were intranasally infected with 4×10^4 PFU of the indicated virus and monitored daily for survival. The data shown are from one experiment representative of two independent experiments with 5 mice/group. The data are presented as means and SEM.

binase (Fig. 1A). rJ-Cre was propagated and analyzed for its ability to replicate in tissue culture cells and to cause lethal encephalitis in mice. Insertion of the *Cre* gene had little to no effect on virus replication in 17Cl-1 cells compared to wild-type rJ (Fig. 1B). Infection of C57BL/6 mice with 4×10^4 rJ-Cre viruses resulted in morbidity and mortality indistinguishable from those seen in mice infected with rJ (Fig. 1C). Together, these results indicate that the insertion of Cre into the rJ genome did not appreciably alter viral fitness.

To assess the functionality of Cre expressed from rJ-Cre, tdTomato mice were intranasally infected with 4×10^4 rJ-Cre viruses. After intranasal infection, rJ accesses the brain by replication in the olfactory receptor neurons and anterograde travel to the neurons of the olfactory bulb. Virus then spreads transneuronally throughout the brain via primary, secondary, and tertiary connections of the OB, reaching sites in the brainstem, amygdala, and midbrain by 7 days postinfection (dpi) (23, 24). In preliminary experiments, we observed that approximately 7 days were required after inoculation of the animal before tdTomato expression was sufficiently elevated to be detected by confocal microscopy. By 11 dpi, robust tdTomato levels could be detected by confocal microscopy in neurons of the olfactory system, including neurons in the brainstem at sites known to be tertiary connections of the OB (Fig. 2A). Periglomerular cells (Fig. 2B, right, arrows) were often degenerate (i.e., nuclei were small and hyperchromatic). These changes were seen on a background of moderate cellular inflammation. These results indicated that, as expected, rJ-Cre expressed Cre recombinase *in vivo* and that expression levels of tdTomato were sufficient for studying cells that survived the acute infection.

tdTomato-expressing cells remain after virus clearance. To determine more precisely the temporal relationship between virus infection and tdTomato positivity, we harvested brains at 4, 7, and 11 dpi and assessed tdTomato and viral nucleocapsid (N) protein expression using confocal microscopy. In preliminary studies, we noted that tdTomato expression lagged behind that of viral antigen, likely reflecting the requirement for Cre expression, transport to the nucleus, DNA excision, and mRNA translation before protein can be expressed. Consequently, we focused our studies on the OB because it is the first site of virus replication. Further, JHMV and other strains of MHV show a preference for replicating in the OB even when virus is introduced intracranially, as virus titers are often highest in this part of the brain (10, 11, 34). After staining OB sections with anti-N monoclonal antibody (MAb) at 4 dpi, neither viral antigen nor

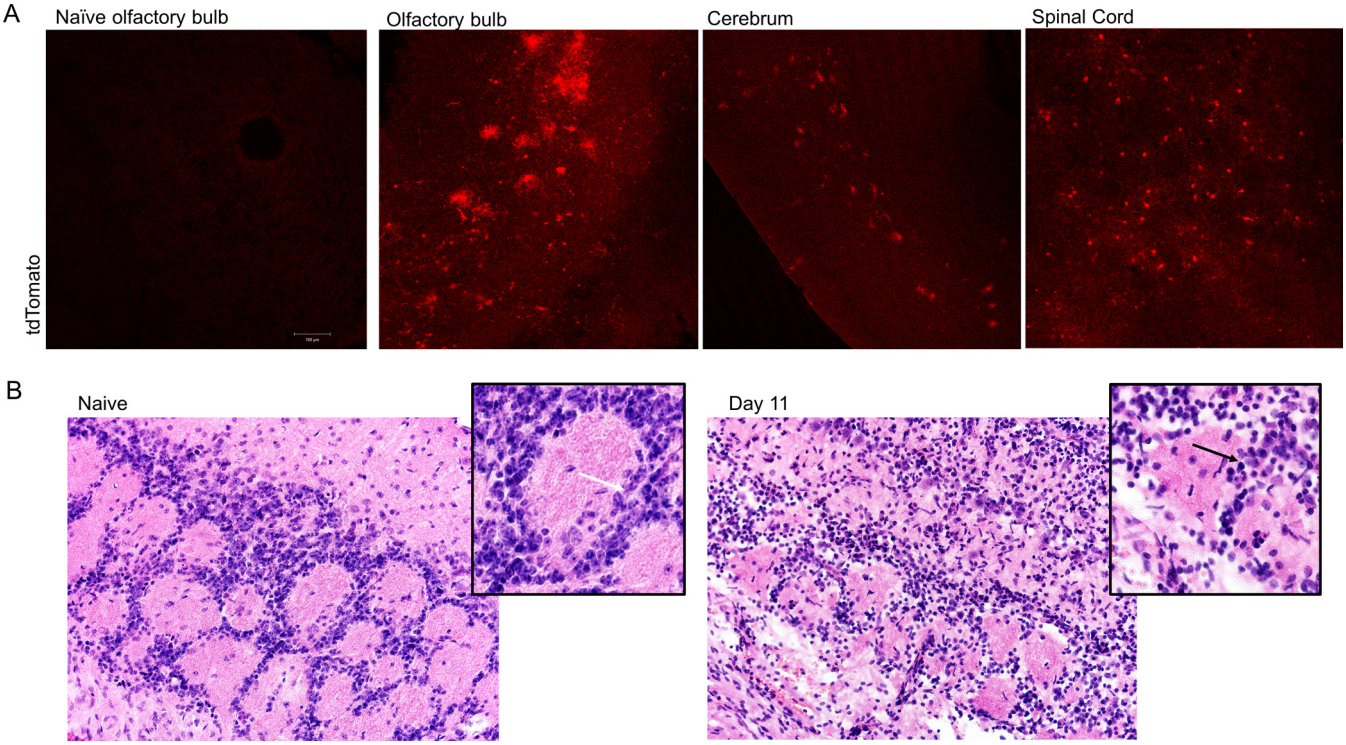

FIG 2 Visualization of tdTomato-positive cells and brain pathology in brains after rJ.Cre infection. (A) Eleven days postinfection, brains from Cre reporter tdTomato mice were harvested, cryosectioned, and imaged without any additional staining. Images are representative of analyses of 7 mice. (B) Histology of olfactory bulbs in naive and rJ-Cre-infected animals at 11 dpi. The white arrow in the inset on the left indicates a healthy periglomerular cell; the black arrow in the inset on the right indicates nuclear changes seen in periglomerular cells. Images are shown at ×10 magnification; however, the insets represent cropped versions of the original images that were magnified to show an individual glomerulus.

tdTomato was detected in the olfactory bulb (Fig. 3A). However, distinct tdTomato$^+$ and N protein$^+$ cells were apparent by 7 dpi. N protein was detected in spite of the increase in autofluorescence seen upon virus infection. At 7 dpi, most tdTomato colocalized with N protein, though some strongly tdTomato$^+$ N protein-negative cells were clearly visible (Fig. 3B). However, by 11 dpi, viral antigen was no longer detected within the OB, even as tdTomato expression became more prominent (Fig. 3A).

As additional support for the notion that the presence of tdTomato$^+$ cells reflected cell survival after virus clearance, we measured levels of viral RNA in the OB. Viral subgenomic RNA within the olfactory bulb was detected at 3 dpi, prior to the detection of virus antigen or tdTomato positivity, and reached peak levels at 5 dpi (Fig. 3C). Levels of subgenomic RNA then declined, and RNA was detected at low levels at 7 dpi, indicating that viral clearance was occurring. The presence of tdTomato-expressing cells in the OB even as virus was cleared from this site supports the conclusion that at least a subset of CNS cells was able to clear the infection and remain viable.

Interneurons of the olfactory bulb survive rJ infection. As expected, given the cellular tropism of rJ, most surviving tdTomato-positive cells were neurons, as demonstrated morphologically and confirmed by NeuroTrace (Thermo Fisher Scientific) staining (Fig. 4). Some neurons within the olfactory bulb strongly expressed tdTomato throughout the cell. As demonstrated by morphology, neurons surviving rJ-Cre infection were largely interneurons (Fig. 4B); no mitral cells were tdTomato positive, perhaps indicating that mitral cells did not survive rJ infection. Surviving interneurons were primarily located in the glomerular cell layer and granule cell layer of the olfactory bulb (Fig. 5A). These results indicate that interneurons comprised a large fraction of the cells that survived rJ infection, suggesting an increased ability to survive the viral infection.

Interneurons of the olfactory bulb are classified based on their location and expression of neurotransmitters and other cell markers. For example, periglomerular interneu-

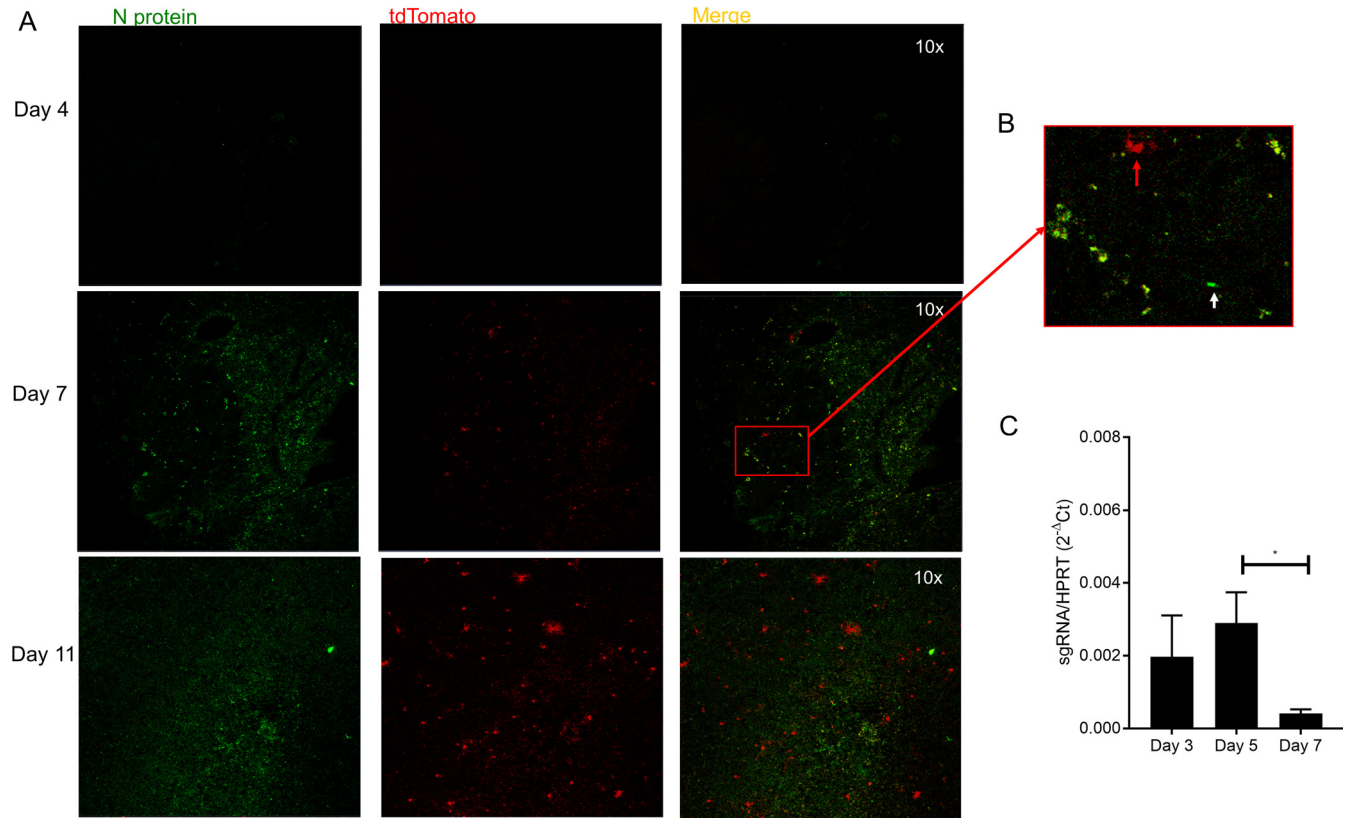

FIG 3 Temporal detection of tdTomato- and N protein-positive cells. (A) Brains from naive and rJ-Cre-infected tdTomato mice were harvested, cryosectioned, and visualized after staining with a monoclonal antibody to the viral N protein at 4, 7, and 11 dpi. All the images are of the olfactory bulb region. (B) Enlargement of the boxed area shown in panel A the red arrow indicates a tdTomato$^+$ N$^-$ cell, while the white arrow indicates a tdTomato$^-$ N$^+$ cell; the remainder of the cells are positive for both tdTomato and N protein. (C) RNA was isolated from the olfactory bulbs of infected mice at the indicated time points. A quantitative-PCR assay was used to determine levels of subgenomic viral RNA. Expression of subgenomic RNA was normalized to HPRT. The data shown represent 4 or 5 mice at each time point.

rons of the glomerular cell layer can be calretinin, tyrosine hydroxylase, or calbindin positive. To define more precisely the type of interneuron surviving rJ-Cre infection, we stained olfactory bulbs with antibodies to tyrosine hydroxylase, calretinin, and parvalbumin. tdTomato-positive cells did not express any of these markers. While readily detected, tyrosine hydroxylase-expressing cells did not coexpress tdTomato (Fig. 5B). Similarly, tdTomato$^+$ parvalbumin$^+$ and tdTomato$^+$ calretinin$^+$ cells also were not detected (Fig. 5C and D). These results suggest that expression of the cell-specific marker was decreased in surviving cells, or alternatively, infection was predominantly of an interneuron subset not expressing one of the three proteins that we assayed.

Rare glial cells survive rJ infection. rJ is known to primarily infect neurons (25, 26), and tdTomato$^+$ cells are morphologically neurons; however, rJ infection of glia has also been reported (28, 35, 36). To better characterize the relative proportions of neuronal and nonneuronal cells in the brain that survive infection, we stained sections from infected tdTomato$^+$ mice with antibodies specific for astrocytes and microglia. First, sections were stained with antibody to glial fibrillary acidic protein (GFAP), a well-described protein expressed by astrocytes. The results showed that few astrocytes were tdTomato$^+$, although a few tdTomato$^+$ astrocytes were found (Fig. 6A). To determine whether microglia survived rJ-Cre infection, we immunostained OB sections with an antibody to IBA-1, a protein that is upregulated on these cells at sites of inflammation. Some cells exhibited colocalization of IBA-1 and tdTomato after infection (Fig. 6B), but the pattern of colocalization appeared punctate and phenotypically different from the diffuse tdTomato expression detected in neurons. Therefore, this punctate pattern may represent microglia/macrophage phagocytosis of tdTomato$^+$ cells as opposed to *de*

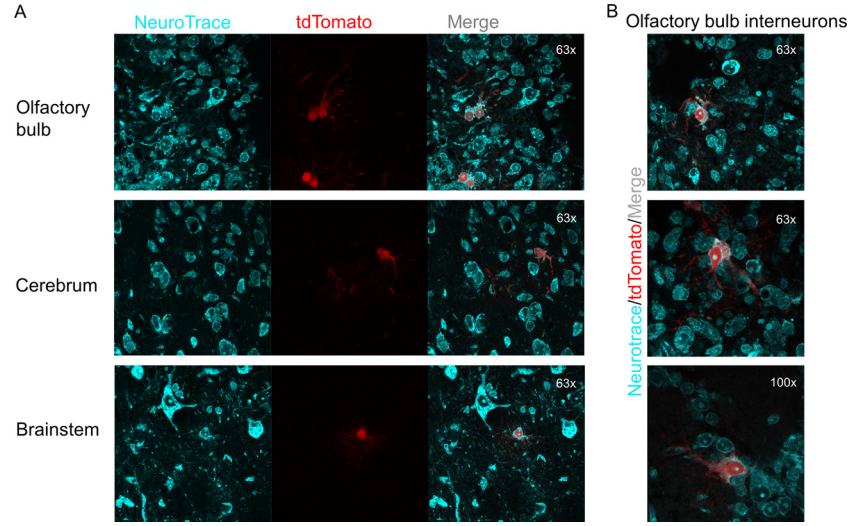

FIG 4 tdTomato-positive cells are largely neurons. (A) rJ-Cre-infected tdTomato mice were euthanized at 11 dpi. Cryosections from the indicated areas of the brain were stained with the fluorescent Nissl stain NeuroTrace. (B) High-power images of olfactory bulb interneurons stained with NeuroTrace. The images are representative of 3 to 5 mice.

novo tdTomato expression. Consistent with this interpretation, there was a lack of tdTomato positivity detected in the nuclei of these cells. To confirm these results, we bred CX3CR1-GFP (green fluorescent protein) mice, which serve as microglial reporter mice, to tdTomato mice. F1 progeny from this cross were infected with rJ-Cre. These mice constitutively express GFP in microglia/macrophages and will express tdTomato in

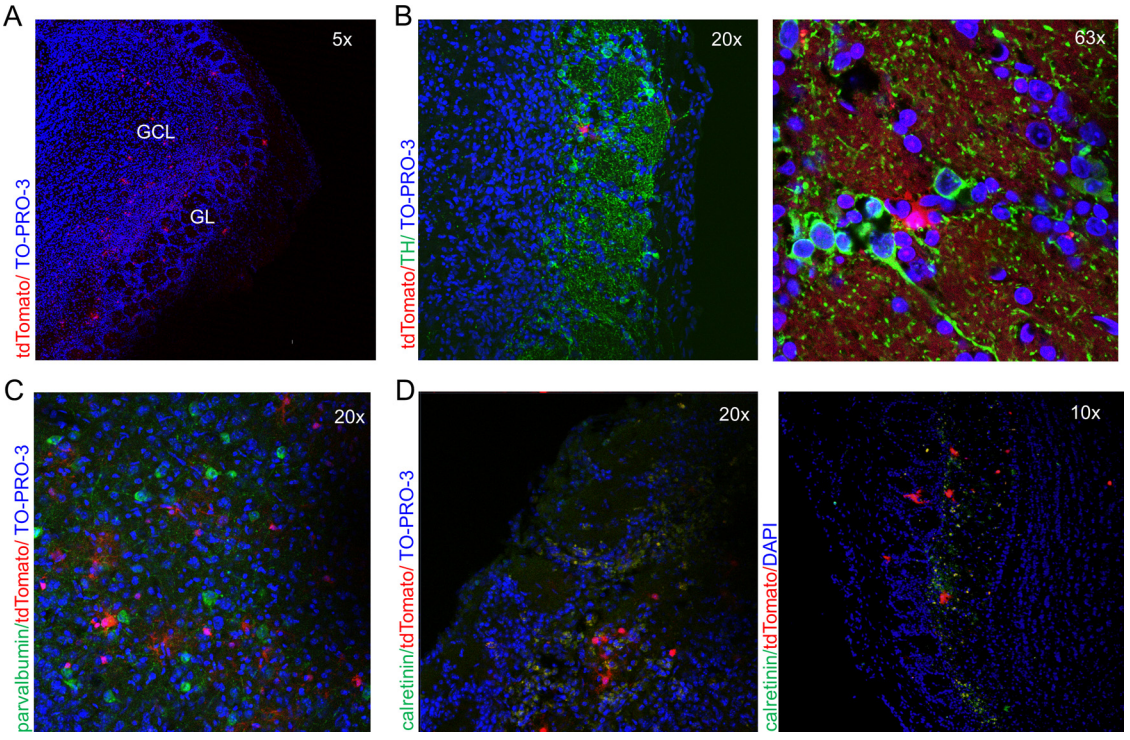

FIG 5 Surviving tdTomato-positive cells in the OB are primarily interneurons. rJ-Cre-infected brains were harvested, cryosectioned, and stained as indicated. (A) Low-power view of the olfactory bulb showing the anatomical location of surviving tdTomato-positive cells. The glomerular layer (GL) and granule cell layer (GCL) are labeled. (B to D) Tyrosine hydroxylase (B), parvalbumin (C), and calretinin (D) antibody staining of cryosectioned olfactory bulbs. All the images are of the olfactory bulb region at 11 dpi and are representative of 3 to 5 mice.

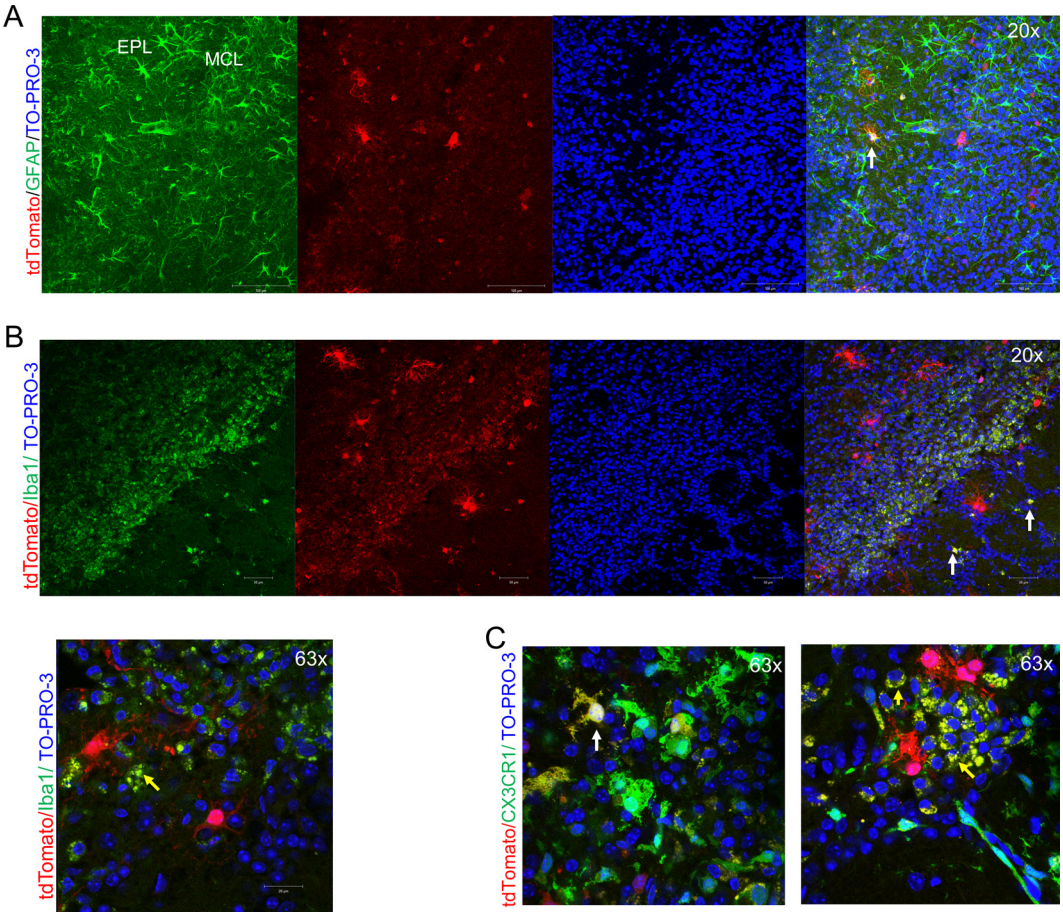

FIG 6 A small fraction of glia is tdTomato positive. Brains from rJ-Cre-infected tdTomato mice were harvested at 11 dpi, cryosectioned, and stained with antibodies to detect astrocytes (GFAP) (A) or microglia (IBA1) (B). (C) Brains from tdTomato$^{+/-}$ CX3CR1$^{GFP/+}$ mice were harvested at 11 dpi, cryosectioned, and visualized after Topro-3 nuclear staining. The yellow arrows indicate punctate tdTomato, CX3CR1-GFP double labeling. (A, B, and C) The white arrows indicate surviving double-labeled cells.

cells after viral infection, eliminating the need for immunostaining. Experiments with CX3CR1$^{GFP/+}$ tdTomato$^{+/-}$ mice largely recapitulated the punctate IBA1 immunostaining described above. Microglia/macrophages with a punctate pattern of tdTomato were near tdTomato^{+} neurons (Fig. 6C). However, uncommon cells with the typical morphology of microglia, showing a more diffuse pattern of tdTomato expression in both the cytoplasm and nucleus, were also found, suggestive of rare endogenous infection (Fig. 6C). Collectively, these results indicate that rJ is capable of infecting glial cells, albeit at low levels, and that some astrocytes and microglia survive rJ infection. They also suggest, perhaps not surprisingly, that microglia/macrophages play a role in clearing virus-infected cells.

DISCUSSION

While the consequences of viral infection in the central nervous system can be devastating because of neuronal loss, little is known about whether neurons that survive are dysfunctional. The main challenge in studying neurons affected by virus infection is to identify and isolate those cells after virus has been cleared. Here, we demonstrate a method useful for identifying previously infected cells by alteration of the host genome using virus-expressed Cre protein. We used a virulent neurotropic CoV that results in a lethal disease by 12 dpi. We found cells, especially in the OB, that survived the infection at times when viral antigen could no longer be detected by immunostaining. These results corroborate previous studies in which populations of

cells that survive infection were identified using Cre-based methodology. In one such study, small numbers of cells, found to be club cells by mRNA sequencing, survived influenza A virus infection and had increased levels of interferon-stimulated proteins, resulting in an inflammatory disease (37). In another study, an attenuated rabies virus-expressing Cre reporter system showed that neurons survived up to 6 months after infection. Surviving neurons in this study showed alterations in transcripts for neuronal function and structure by microarray analysis (29). Our results using a virulent strain of JHMV indicate that neurons can even survive infection with a highly pathogenic virus.

Our results provide proof of principle for using a Cre reporter model for studying cells surviving MHV infection in the central nervous system. Additionally, GFAP and IBA1 staining confirmed that neurons preferentially survive rJ infection, since few astrocytes or microglia expressed tdTomato after infection. These results are consistent with previous work demonstrating tropism for neuronal cells, but it is also possible that glial cells survive infection less frequently. Future work based on the method described here will be useful for studying the CNS of mice infected with CoV with different cellular tropisms. Of particular interest will be the consequences of infection with the neuroattenuated J2.2-V-1 strain of JHMV, which preferentially infects oligodendrocytes and causes clinically apparent demyelinating disease. A Cre-expressing recombinant J2.2 would allow study of the effects of viral infection on oligodendrocyte RNA and protein expression and would provide new information on the effects of prior infection on demyelination and remyelination. Most studies have focused on gross areas of myelin destruction, but such a recombinant virus would facilitate analyses of surviving and possibly dysfunctional cells.

Many viruses replicate in the nasal cavity and the olfactory epithelium, which is distinct from the respiratory epithelium, and serves as an important portal of virus entry into the CNS (1). Thus, virus is first detected in the OB in experimental infections caused by neurotropic influenza A virus, West Nile virus, and others (2–6). In a similar vein, the OBLV strain of MHV replicates to high titers in the OB, with little evidence of spread elsewhere in the brains of immunocompetent mice (10, 11, 34). However, in mice lacking T or B cells, OBLV spreads throughout the brain (34). The propensity for viruses to invade the CNS via the OB, combined with the uncommonness of viral encephalitis, suggests that the olfactory epithelium, nerve, or bulb may limit viral spread to and within the CNS, perhaps by modulating the immune response. Our results indicate that some cells in the OB, especially interneurons, survive the initial virus infection. These cells are primarily inhibitory and modulate neuronal function. Whether these surviving neurons have diminished function resulting in changes in olfaction will require additional investigation.

MATERIALS AND METHODS

Cell culture. MHV receptor-expressing HeLa cells (HeLa-MHVR), 17Cl-1 cells, and MHV receptor-expressing BHK cells were grown as previously described (38, 39).

Generation of recombinant JHMV-Cre. Cre recombinase was cloned into pBAC-JHMV as previously described (31). Briefly, a PCR product containing Cre–FLP recombination target (FRT)–kanamycin resistance cassette (Kan^r)–FRT and 5′ and 3′ homology to the regions just outside ORF4 was created using two-step PCR. A plasmid containing Cre sequence was a gift from Benjamin tenOever (Icahn School of Medicine). This cassette was transformed into *Escherichia coli* containing pBAC-JHMV^{IA}. Bacteria with successfully recombined pBAC-JHMV were identified by kanamycin resistance. Correct clones were amplified and treated with Flp recombinase to excise the kanamycin resistance cassette surrounded by Flp recombination targets. pBAC-derived JHMV-Cre was obtained after transfection as previously described (31). rJ-Cre virus was grown on 17Cl-1 cells, and virus titers were determined on HeLa-MHVR cells (40). 17Cl-1 cells were infected with rJ at a multiplicity of infection (MOI) of 0.1, and virus from the supernatant and cells was combined prior to determining viral titers. Virus was passaged five times to obtain sufficient stocks to use in mouse experiments and an additional three times to assess the stability of the Cre insertion. Levels of Cre expression were unchanged through 7 passages but were diminished by passage 8, indicating some instability of the Cre gene.

Mice. Specific-pathogen-free C57BL/6 mice were purchased from Charles River. B6.Cg-*Gt*(*ROSA*)*26Sor*$^{tm14(CAG-tdTomato)Hze}$/J (tdTomato) mice were purchased from Jackson Laboratories. B6.129P(Cg)-*Ptprc*^{a} *Cx3cr1*^{tm1Litt}/LittJ (CX3CR1-GFP) mice were also purchased from Jackson Laboratories and bred to tdTomato mice. The mice were maintained in specific-pathogen-free facilities at the University of Iowa.

Male mice were used in all experiments. Five- to 6-week-old mice were intranasally inoculated with 40,000 PFU rJHM-Cre after isoflurane anesthesia. After viral inoculation, the mice were observed and weighed daily. To determine the titer of virus from infected animals, mice were sacrificed and perfused with phosphate-buffered saline (PBS). Brain tissue was homogenized into PBS using a manual homogenizer and frozen. After thawing, cellular debris was removed by centrifugation, and virus titers in the supernatant were determined on HeLa-MHVR cells. The University of Iowa Institutional Animal Care and Use Committee approved all mouse experiments.

RNA analysis. Olfactory bulbs were collected at the indicated times and placed into TRIzol (Thermo Fisher Scientific). RNA was isolated according to the manufacturer's instructions. The RNA was transcribed into cDNA using Moloney murine leukemia virus reverse transcriptase (MMLV RT) (Thermo Fisher Scientific). Subgenomic RNA levels were measured on a QuantStudio qPCR 3 system (Thermo Fisher Scientific) using previously described subgenomic RNA primers (41). The levels of subgenomic RNA were normalized to hypoxanthine-guanine phosphoribosyltransferase (HPRT) by the following threshold cycle (C_T) equation: $\Delta C_T = C_T$ of gene of interest $- C_T$ of HPRT. All results are shown as a ratio to HPRT calculated as $2^{-\Delta CT}$.

Tissue processing. After perfusion of the mice, their brains were transferred to 4% paraformaldehyde solution at a 20:1 volume-to-weight ratio. After 48 h, the brains were cryoprotected by immersion in 10% sucrose for 30 min, followed by immersion in 20% sucrose for several hours until the brains had dropped to the bottom of the solution. Then, the brains were transferred to 30% sucrose and kept at 4°C overnight. The brains were snap-frozen in tissue-freezing medium using a standalone Gentle Jane device (Instrumedics, Inc.). Ten- or 50-μm sections were obtained on a Thermo cryostat and stored at −80°C. For hematoxylin and eosin (H&E) staining, brains were removed, fixed in zinc formalin, and then embedded in paraffin. Tissue sections were stained with H&E.

Tissue staining and imaging. For staining, frozen sections were warmed at room temperature for 10 min. The sections were immersed in PBS for 10 min before a 10-min treatment with 0.1% Triton X in PBS. The sections were then rinsed in PBS 3 times for 5 min each time. Next, samples were incubated in CAS block (Invitrogen) for 10 min, followed by incubation in primary antibody diluted in 1% goat serum in PBS overnight at 4°C in a humidity chamber. Primary antibodies to GFAP (Sigma) at 1:10,000, IBA1 (Wako) at 1:2,000, parvalbumin (Sigma) at 1:1,000, tyrosine hydroxylase (Millipore) at 1:1,000, calretinin (Millipore) at 1:1,000, and viral N protein (kindly provided by Michael Buchmeier, University of California, Irvine, CA) at 1:10,000 were used. The sections were rinsed before incubation with a 1:200 dilution of an appropriate A488-conjugated goat anti-mouse or anti-rabbit antibody (Thermo Fisher Scientific). In some cases, Topro-3 (Thermo Fisher Scientific) was included in the secondary-antibody staining solution at a 1:1,000 dilution. After rinsing with PBS, the slides were mounted with Vectashield antifade reagent (Vectashield Laboratories); in some experiments, Vectashield containing DAPI (4′,6-diamidino-2-phenylindole) was used. NeuroTrace staining was performed following the manufacturer's protocol. Images were obtained using a Zeiss LSM510 confocal microscope or an Olympus BX61 light microscope.

Statistics. Data are presented as means and standard errors of the mean (SEM) unless otherwise indicated. Mann-Whitney *U* tests were used to analyze differences in means. Log-rank tests were used to determine significant differences in survival of mice. *P* values of <0.05 were considered significant.

ACKNOWLEDGMENTS

We thank Anthony Fehr and Alan Sariol for critical reviews of the manuscript. We acknowledge use of the University of Iowa Central Microscopy Research Facility.

The work was supported in part by grants from the NIH (N36592) and National Multiple Sclerosis Society (RG 5340-A-7). The University of Iowa Central Microscopy Research Facility is a core resource supported by the Vice President for Research and Economic Development, the Holden Comprehensive Cancer Center, and the Carver College of Medicine.

REFERENCES

1. van Riel D, Verdijk R, Kuiken T. 2015. The olfactory nerve: a shortcut for influenza and other viral diseases into the central nervous system. J Pathol 235:277–287. https://doi.org/10.1002/path.4461.
2. Majde JA, Bohnet SG, Ellis GA, Churchill L, Leyva-Grado V, Wu M, Szentirmai E, Rehman A, Krueger JM. 2007. Detection of mouse-adapted human influenza virus in the olfactory bulbs of mice within hours after intranasal infection. J Neurovirol 13:399–409. https://doi.org/10.1080/13550280701427069.
3. Leyva-Grado VH, Churchill L, Harding J, Krueger JM. 2010. The olfactory nerve has a role in the body temperature and brain cytokine responses to influenza virus. Brain Behav Immun 24:281–288. https://doi.org/10.1016/j.bbi.2009.10.007.
4. Mori I, Nishiyama Y, Yokochi T, Kimura Y. 2005. Olfactory transmission of neurotropic viruses. J Neurovirol 11:129–137. https://doi.org/10.1080/13550280590922793.
5. Faber HK, Gebhardt LP. 1933. Localizations of the virus of poliomyelitis in the central nervous system during the preparalytic period, after intranasal instillation. J Exp Med 57:933–954. https://doi.org/10.1084/jem.57.6.933.
6. Monath TP, Cropp CB, Harrison AK. 1983. Mode of entry of a neurotropic arbovirus into the central nervous system. Reinvestigation of an old controversy. Lab Invest 48:399–410.
7. Yamagishi M, Fujiwara M, Nakamura H. 1994. Olfactory mucosal findings and clinical course in patients with olfactory disorders following upper respiratory viral infection. Rhinology 32:113–118.
8. Yamagishi M. 1988. Immunohistochemical study of the olfactory epithelium in the process of regeneration. Nihon Jibiinkoka Gakkai Kaiho 91:730–738.
9. Moran DT, Jafek BW, Eller PM, Rowley JC III. 1992. Ultrastructural histopathology of human olfactory dysfunction. Microsc Res Tech 23:103–110. https://doi.org/10.1002/jemt.1070230202.
10. Youngentob SL, Schwob JE, Saha S, Manglapus G, Jubelt B. 2001. Func-

tional consequences following infection of the olfactory system by intranasal infusion of the olfactory bulb line variant (OBLV) of mouse hepatitis strain JHM. Chem Senses 26:953–963. https://doi.org/10.1093/chemse/26.8.953.
11. Schwob JE, Saha S, Youngentob SL, Jubelt B. 2001. Intranasal inoculation with the olfactory bulb line variant of mouse hepatitis virus causes extensive destruction of the olfactory bulb and accelerated turnover of neurons in the olfactory epithelium of mice. Chem Senses 26:937–952. https://doi.org/10.1093/chemse/26.8.937.
12. Murthy VN. 2011. Olfactory maps in the brain. Annu Rev Neurosci 34:233–258. https://doi.org/10.1146/annurev-neuro-061010-113738.
13. Lodovichi C, Belluscio L. 2012. Odorant receptors in the formation of the olfactory bulb circuitry. Physiology (Bethesda) 27:200–212. https://doi.org/10.1152/physiol.00015.2012.
14. Nagayama S, Homma R, Imamura F. 2014. Neuronal organization of olfactory bulb circuits. Front Neural Circuits 8:98. https://doi.org/10.3389/fncir.2014.00098.
15. Bagley J, LaRocca G, Jimenez DA, Urban NN. 2007. Adult neurogenesis and specific replacement of interneuron subtypes in the mouse main olfactory bulb. BMC Neurosci 8:92. https://doi.org/10.1186/1471-2202-8-92.
16. Merkle FT, Fuentealba LC, Sanders TA, Magno L, Kessaris N, Alvarez-Buylla A. 2014. Adult neural stem cells in distinct microdomains generate previously unknown interneuron types. Nat Neurosci 17:207–214. https://doi.org/10.1038/nn.3610.
17. Parrish-Aungst S, Shipley MT, Erdelyi F, Szabo G, Puche AC. 2007. Quantitative analysis of neuronal diversity in the mouse olfactory bulb. J Comp Neurol 501:825–836. https://doi.org/10.1002/cne.21205.
18. Batista-Brito R, Close J, Machold R, Fishell G. 2008. The distinct temporal origins of olfactory bulb interneuron subtypes. J Neurosci 28:3966–3975. https://doi.org/10.1523/JNEUROSCI.5625-07.2008.
19. Lledo PM, Merkle FT, Alvarez-Buylla A. 2008. Origin and function of olfactory bulb interneuron diversity. Trends Neurosci 31:392–400. https://doi.org/10.1016/j.tins.2008.05.006.
20. Perlman S, Netland J. 2009. Coronaviruses post-SARS: update on replication and pathogenesis. Nat Rev Microbiol 7:439–450. https://doi.org/10.1038/nrmicro2147.
21. Compton SR, Barthold SW, Smith AL. 1993. The cellular and molecular pathogenesis of coronaviruses. Lab Anim Sci 43:15–28.
22. Bergmann CC, Lane TE, Stohlman SA. 2006. Coronavirus infection of the central nervous system: host-virus stand-off. Nat Rev Microbiol 4:121–132. https://doi.org/10.1038/nrmicro1343.
23. Barnett EM, Perlman S. 1993. The olfactory nerve and not the trigeminal nerve is the major site of CNS entry for mouse hepatitis virus, strain JHM. Virology 194:185–191. https://doi.org/10.1006/viro.1993.1248.
24. Barnett EM, Cassell MD, Perlman S. 1993. Two neurotropic viruses, herpes simplex virus type 1 and mouse hepatitis virus, spread along different neural pathways from the main olfactory bulb. Neuroscience 57:1007–1025. https://doi.org/10.1016/0306-4522(93)90045-H.
25. Dubois-Dalcq ME, Doller EW, Haspel MV, Holmes KV. 1982. Cell tropism and expression of mouse hepatitis viruses (MHV) in mouse spinal cord cultures. Virology 119:317–331. https://doi.org/10.1016/0042-6822(82)90092-7.
26. Knobler RL, Dubois-Dalcq M, Haspel MV, Claysmith AP, Lampert PW, Oldstone MB. 1981. Selective localization of wild type and mutant mouse hepatitis virus (JHM strain) antigens in CNS tissue by fluorescence, light and electron microscopy. J Neuroimmunol 1:81–92. https://doi.org/10.1016/0165-5728(81)90010-2.
27. Knobler RL, Tunison LA, Lampert PW, Oldstone MB. 1982. Selected mutants of mouse hepatitis virus type 4 (JHM strain) induce different CNS diseases. Pathobiology of disease induced by wild type and mutants ts8 and ts15 in BALB/c and SJL/J mice. Am J Pathol 109:157–168.
28. Fleming JO, Trousdale MD, el-Zaatari FA, Stohlman SA, Weiner LP. 1986. Pathogenicity of antigenic variants of murine coronavirus JHM selected with monoclonal antibodies. J Virol 58:869–875.
29. Gomme EA, Wirblich C, Addya S, Rall GF, Schnell MJ. 2012. Immune clearance of attenuated rabies virus results in neuronal survival with altered gene expression. PLoS Pathog 8:e1002971. https://doi.org/10.1371/journal.ppat.1002971.
30. Madisen L, Zwingman TA, Sunkin SM, Oh SW, Zariwala HA, Gu H, Ng LL, Palmiter RD, Hawrylycz MJ, Jones AR, Lein ES, Zeng H. 2010. A robust and high-throughput Cre reporting and characterization system for the whole mouse brain. Nat Neurosci 13:133–140. https://doi.org/10.1038/nn.2467.
31. Fehr AR, Athmer J, Channappanavar R, Phillips JM, Meyerholz DK, Perlman S. 2015. The nsp3 macrodomain promotes virulence in mice with coronavirus-induced encephalitis. J Virol 89:1523–1536. https://doi.org/10.1128/JVI.02596-14.
32. Ontiveros E, Kuo L, Masters PS, Perlman S. 2001. Inactivation of expression of gene 4 of mouse hepatitis virus strain JHM does not affect virulence in the murine CNS. Virology 289:230–238. https://doi.org/10.1006/viro.2001.1167.
33. Ontiveros E, Kuo L, Masters P, Perlman S. 2001. Analysis of nonessential gene function in recombinant MHV-JHM. Gene 4 knockout recombinant virus. Adv Exp Med Biol 494:83–89. https://doi.org/10.1007/978-1-4615-1325-4_13.
34. Pearce BD, Hobbs MV, McGraw TS, Buchmeier MJ. 1994. Cytokine induction during T-cell-mediated clearance of mouse hepatitis virus from neurons in vivo. J Virol 68:5483–5495.
35. Weiner LP. 1973. Pathogenesis of demyelination induced by a mouse hepatitis. Arch Neurol 28:298–303. https://doi.org/10.1001/archneur.1973.00490230034003.
36. Sun N, Perlman S. 1995. Spread of a neurotropic coronavirus to spinal cord white matter via neurons and astrocytes. J Virol 69:633–641.
37. Heaton NS, Langlois RA, Sachs D, Lim JK, Palese P, ten Oever BR. 2014. Long-term survival of influenza virus infected club cells drives immunopathology. J Exp Med 211:1707–1714. https://doi.org/10.1084/jem.20140488.
38. Yount B, Denison MR, Weiss SR, Baric RS. 2002. Systematic assembly of a full-length infectious cDNA of mouse hepatitis virus strain A59. J Virol 76:11065–11078. https://doi.org/10.1128/JVI.76.21.11065-11078.2002.
39. Zhou H, Perlman S. 2007. Mouse hepatitis virus does not induce beta interferon synthesis and does not inhibit its induction by double-stranded RNA. J Virol 81:568–574. https://doi.org/10.1128/JVI.01512-06.
40. Pewe L, Zhou H, Netland J, Tangudu C, Olivares H, Shi L, Look D, Gallagher T, Perlman S. 2005. A severe acute respiratory syndrome-associated coronavirus-specific protein enhances virulence of an attenuated murine coronavirus. J Virol 79:11335–11342. https://doi.org/10.1128/JVI.79.17.11335-11342.2005.
41. Athmer J, Fehr AR, Grunewald M, Smith EC, Denison MR, Perlman S. 2017. In situ tagged nsp15 reveals interactions with coronavirus replication/transcription complex-associated proteins. mBio 8:e02320-16. https://doi.org/10.1128/mBio.02320-16.